Proceedings World Geothermal Congress 2020+1
Reykjavik, Iceland, April - October 2021

Scalings in Geothermal Systems

Bernhard Köhl and Thomas Baumann

Chair of Hydrogeology, Technical University of Munich, Arcisstr. 21, 80333 München, Germany

tbaumann@tum.de

Keywords: Scalings, Molasse Basin, carbonates, hydrogeochemical model

ABSTRACT

The majority of scalings observed at geothermal facilities exploring the Malm Aquifer in the Bavarian Molasse Basin are carbonates. They are formed due to a disruption of the lime-carbonic-acid equilibrium during production caused by degassing of carbon dioxide. These scalings are found in the production pipes, at the pumps and at filters and can nicely be described using existing hydrogeochemical models.

In order to mitigate those scalings, the process of scaling formation and the influencing factors have to be better understood. Therefore, scalings of all sections of geothermal facilities have been taken. The database consists of scaling samples from 13 geothermal pumps, 6,000 m production pipe (sample interval 10-12 m), 11 evaporator revisions, 2 injection pipes and numerous filter elements. The samples were analyzed by SEM-EDX, XRD, Raman spectroscopy and acid digestion to assess their chemical and mineralogical composition.

The development of scalings directly above the pumps correlates with the number of startup cycles. Precipitation closer to ground level is rate limited. Scalings in the production pipes become critical if they are detached by hydraulic or thermal stress. Scalings observed in ground level facilities were traced back to residues of the cleaning procedure and caused additional downtime. At the injection wells degassing causes high scaling rates. The developed hydrogeochemical models are able to predict the occurrence of scalings and to assess mitigation measures.

1. INTRODUCTION

Geothermal exploration of the Upper Jurassic sediments in the Bavarian Molasse Basin is a success story. There are currently 23 projects in operation with five projects also producing electrical energy. Many of the projects, mainly district heating plants, are running smoothly and with little interruption. However, at the more ambitious projects producing electrical energy, down times due to failures in the thermal water cycle are more often. These projects are usually running at higher temperatures and with higher flow rates. On the other side, geothermal power plants, especially when coupled to a district heating network, are run at steady state conditions: more electricity is produced if the heat demand is low.

Previous investigations (eg. Boch et al. 2015, Wanner et al. 2017) and models (Baumann et al. 2017) show that precipitations can be traced back to a disruption of the lime-carbonic acid equilibrium. The geothermal water is dominated by calcium, magnesium and bicarbonate (Ca-Mg-HCO_3-type). At some locations ion exchange affected the waters significantly (Na-Ca-HCO_3-type) and at other locations waters infiltrating from higher strata lead to an increase of the sodium and chloride concentrations. The concentration of total dissolved solids is usually below 2 g/L. The wells to the west show high gas concentrations up to 2 L gas per L of thermal water and a CH4 to N2 ratio of 12:1. Below and southeast of Munich the gas concentrations are in a range of 200 mL/L and a CH4:N2 ratio of 1:1 is typical. Gas concentrations are varying widely and so does the bubble point (Mayrhofer et al. 2014). Modeling results indicate that a temperature increase at the motors of the submersible pumps and degassing are the main factors controlling the disruption of the hydrochemical equilibria.

While the model performance for forensic investigations of discovered precipitates and for qualitative predictions is very good, the quantitative prediction capabilities leave room for optimization. Scaling potential and observed scaling masses differ significantly, therefore, a predictive maintenance of pumps or pipes is not possible. This is partly due to a lack of experimental field data. Here, we present an excerpt of an extended data set covering precipitates from several kilometers of production pipes, motors, pumps, filters, heat exchangers, and further surface level facilities. The data is complemented by caliber logs and precipitates recovered from the production and injection pipes. The history of most samples is available, therefore, the kinetics of the precipitation is accessible.

2. METHODS

Samples were collected during maintenance of the geothermal facilities covering the different hydrogeochemical regions in the Molasse Basin. Samples were registered, packed individually and stored for further analyses. SEM-EDX was the work horse for the characterization of the precipitates, providing both, morphological data, element spectra and image data of the microstructure, which were later quantitatively processed using ImageJ. Mineralogical data was validated using XRD and Raman spectroscopy.

The hydrogeochemical model is built based on PhreeqC, version 3.15.0, and the included phreeqc.dat database (Parkhurst and Appelo, 2013). The chemical composition and gas analyses of the simulated thermal water are back calculated to reservoir conditions as shown in Baumann, 2016. To simulate degassing in the pump, the pressure in the simulation is set to a value below the bubble point and the composition and volume of the gas phase is calculated with PhreeqC. Solution chemistry and gas phase are read by python script which handles all further calculations. The gas phase is distributed on gas bubbles with a defined initial diameter and is allowed to dissolve based on the kinetic model of Holocher et al., 2003 and taking the hydrostatic pressure after the

pump into account. With this data a PhreeqC input file involving kinetic precipitation of calcite is constructed. Python triggers the simulation with the new input file and reads the results. With a time step of 1 s this procedure is repeated until the well head is reached. The python script allows parameter and sensitivity studies.

3. RESULTS

Figure 1 shows a typical development of the precipitation rates along a production pipe. The precipitates start above the pump and increase to the well head to 1-5 µmol/(m² s). The scaling rates are similar for although the produced volumes differ by a factor of 3. This might indicate, that there is little change of the effective surface area (plain tube wall vs. precipitates on the wall). The rates are on the order of published rate constants for Calcite indicating rate limiting conditions. This makes sense because the flow velocities in the production pipes favor turbulent flow. This and the negligible change of the solution chemistry while the water is in the pipe point to a constant concentration boundary condition at the interface between pipe and water.

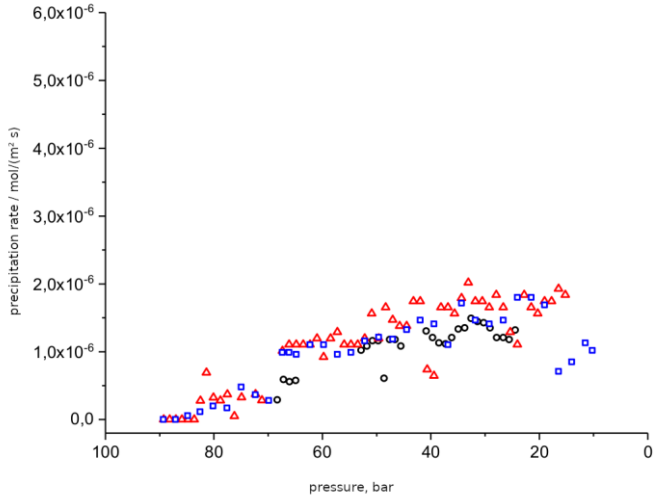

Figure 1: Development of precipitation rates as a function of pressure. Data from three different time intervals with produced volumes between 3 million m³ and 8.5 million m³.

The experimental results show that only the initial scaling rates are depending on the surface properties of the production pipes. Smooth surfaces and polymer coated surfaces show less growth at very early stages. Here, shear forces are big enough to remove larger particles from the surface. However, the applied polymer coating also affects the adherence of the scalings when subjected to thermal or mechanical stress. The recovered pipes clearly show that scalings on coated pipes can be easily detached. Thermal and mechanical stress, eg. during a shutdown of the power plant, will cause the scalings to break off the pipe walls and settle above or in the pump (see Figures 2 and 3). The effects of this accumulation are much more severe than the small pressure losses caused by the attached scalings.

Figure 2: Images of detached precipitates in the production pipe.

Figure 3: Images of scalings at and inside submersible pumps.

Rate limitation alone does not explain the thickness of the precipitates which is increasing from pump to well head. The pressure at the well head and in the surface level facilities is kept above the calculated bubble pressure including a safety margin. Although degassing should not happen at these conditiuons, gas bubbles have been observed through portholes at several parts of the facility (see. Figure 4). This indicates pressures below the bubble point at some place between pump and well head.

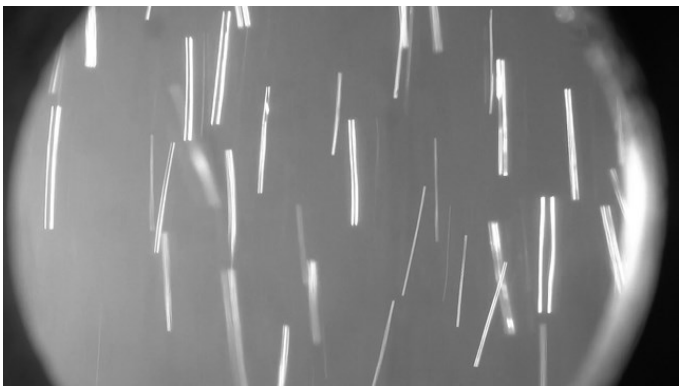

Figure 4: Gas bubbles in the thermal water captured through a porthole at the entrace to the geothermal power plant.

At one facility we observed thick scalings directly above the pump which had a pumice like structure with almost circular pores (Figure 5). The matrix was calcium carbonate, mainly calcite with few vaterite crystals. Such precipitates indicate fast precipitation from supersaturated solution with little time for crystal growth. The thickness of these precipitations decreased to zero at about 400 m above the pump. From here on the scalings also found at other sites started to grow and reached a precipitation rate at the well head which was in the range of other sites. The thickness of the precipitates above the pump is correlated with number of starting cycles of the pump which gives a hint to the underlying precipitation process. When the pump is started, the water column in the bore hole and in the production pipes has to be accelerated from zero to 1.4 m/s causing turbulence, cavitation and degassing. Directly above the pump a multiphase system (gas, thermal water, oil) develops and causes supersaturation due to stripping of CO_2 from the water phase. This happens rapidly and leads to the pumice like scalings. As the pump is producing regularly, the number of gas bubbles is decreasing. This is supported by the data obtained from sites with constant operation.

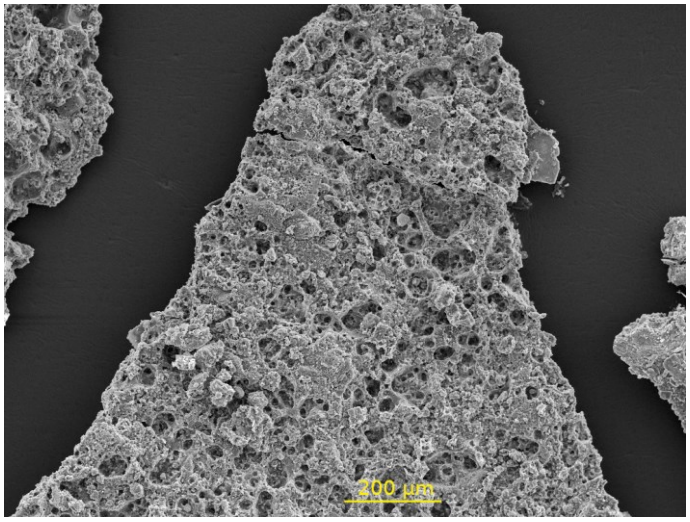

Figure 5: Precipitates from a production pipe directly above the submersible pump.

The process leading to the precipitates directly above the pump might also explain the development of the scaling thickness: we start assuming that gas bubbles are forming inside the pumps. This is supported by observation of cavitation pittings at the impellers and by the technicians of the pump manufacturers. The gas bubbles will leave the pump and enter the production pipe. Here, the pressure is higher than in the pump and the bubbles will shrink. While some gas bubbles will collapse completely, others will get tiny. As the water is produced, the pressure is decreasing allowing the gas bubbles to grow. With bubble growth, CO_2 is stripped from the water and the solution gets more supersaturated. This leads to increasing precipitation rates at the well head. Figure 6 shows the results of a hydrogeochemical model including gas bubble formation and rate limited gas exchange between gas bubble and solution. The observed trend is reproduced qualitatively. The parameter study suggests, that the precipitation rates directly above the pump are controlled by the initial gas bubble size. Larger bubbles increase the scaling rates at this position. The overall scaling rates depend on the area per volume of water. The modeled and measured precipitation rates are similar, however the area per volume of water used in the model is much smaller compared to the theoretical values. This result indicates that only a small, but changing part of the water contributes to scaling formation. During production other parts of the water come in contact with the pipe walls and are allowed to interact. This makes sense considering the fluid dynamics in the production pipes. While some of the experimental data points to a stagnation of the scaling rates closer to the well head, the model predicts increasing scaling rates. Also larger and well formed crystals close to the well head point to lower oversaturation and slower crystal growth. A possible explanation for this discrepancy is film flow at the pipe walls in the uppermost part of the production pipes. Here, the effects of precipitation on the solution chemistry in the film cannot be neglected and this is not yet included in the model. Nevertheless, the incorporation of bubble formation and dissolution is another step towards a predictive model. Modeling results indicate, that small scale interactions at the pipe walls (eg. local degassing in pores, film flow, and shear forces) have to be incorporated into the system.

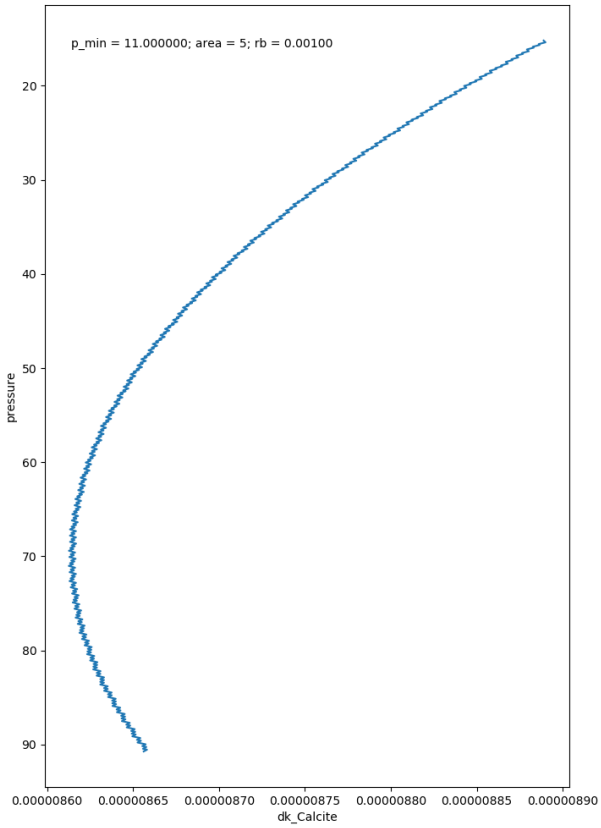

Figure 6: Scaling rates in mol/(m² s) for a geothermal power plant simulated using bubble dissolution; p_min is the minimum pressure in the pump, area is the specific surface area in cm²/L in the kinetic calculations and rb is the initial diameter of the bubbles

4. CONCLUSION

Current theoretical frameworks and models allow a forensic assessment of precipitations in geothermal systems. However, the models are limited with regard to their quantitative predictions. This is not caused by an incomplete model framework, but by a lack of data and ill defined boundary conditions. Further research has to focus on better monitoring data from different parts of the geothermal facility and a better definition of the conditions in the pumps, heat exchangers, and injection pipes. This also requires efforts for sensor development.

The risks caused by scalings at different parts of the geothermal cycle cover a wide range. Attached scalings in the production pipes are acceptable, because their effects on the pressure required for production is negligible. In contrast, precipitates on the motor are becoming fatal, because they limit heat dissipation from the motor and lead to overheating. It seems not to be a good idea to prevent precipitates in production pipes by modified pipe surfaces like polymer claddings or polished surfaces, because the scalings are likely to detach at a later stage and cause damages. Measures to prevent or reduce precipitates at the motor casing makes more sense, because the scalings adversely affect the cooling of the motor.

ACKNOWLEDGMENTS

This work was funded within the project Geothermal-Alliance Bavaria, subproject “Safety of the Thermal Water Cycle” by the “Bayerisches Staatsministerium für Unterricht und Kultus”.

REFERENCES

Baumann, T.: Validation of Hydrochemical Analyses and Gas Concentrations of Deep Geothermal Aquifers. *Proceedings*, 41st Workshop on Geothermal Reservoir Engineering Bd. SGP-TR-209, Stanford University (2016).

Baumann, T., Bartels, J., Lafogler, M., and Wenderoth, F.: Assessment of Heat Mining and Hydrogeochemical Reactions With Data from a Former Geothermal Injection Well in the Malm Aquifer, Bavarian Molasse Basin, Germany. *Geothermics* **66** (2017), S. 50–60

Boch, R., Leis A., Haslinger E., Goldbrunner, J. E., Mittermayr, F., Fröschl, H., Hippler, D. and Dietzel, M., Scale-Fragment Formation Impairing Geothermal Energy Production: Interacting H_2S Corrosion and $CaCO_3$, *Geothermal Energy* **5** (2017), doi:10.1186/s40517-017-0062-3.

Holocher, J., Peeters, F., Aeschbach-Hertig, W., Kinzelbach, W., and Kipfer, R.: Kinetic Model of Gas Bubble Dissolution in Groundwater and Its Implications for the Dissolved Gas Composition. *Environ. Sci. Technol.* **37** (2003) 1337-1343.

Mayrhofer, C., Niessner, R., and Baumann, T.: Hydrochemistry and Hydrogen Sulfide Generating Processes in the Malm Aquifer, Bavarian Molasse Basin, Germany. *Hydrogeol J*. **22** (2014), 151–162.

Parkhurst, D. L. and Appelo, C. A. J.: Description of input and examples for PHREEQC version 3 -- A Computer Program for Speciation, Batch-Reaction, One-Dimensional Transport, and Inverse Geochemical Calculations, U.S. Geological Survey, Techniques and Methods 6-A43 (2013).

Wanner, C., Eichinger, F., Jahrfeld, T., and Diamond, L.: Causes of Abundant Calcite Scaling in Geothermal Wells in the Bavarian Molasse Basin, Southern Germany, *Geothermics* **70** (2017), 324-338.